Chapter 2

STRUCTURES AND REACTIVITY PATTERNS OF GROUP 9 METALLOCORROLES

In "Iridium Corroles," I detailed the synthesis, characterization, and electrochemical properties of the corroles **1-Ir(tma)$_2$** and **1b-Ir(tma)$_2$**. I also assigned the lower-potential redox process in these systems to a metal-based oxidation, claiming that corroles, because of their powerful sigma-donating properties, have a unique ability to stabilize higher-valent transition metal ions. Having the first fully characterized set of third-row metallocorroles in hand, I wanted to compare their properties with those of more well-studied first and second row metallocorrole derivatives. The first order of business was to develop syntheses for Ir(III) corroles analogous to known Co(III) and Rh(III) derivatives. Since the pyridine- and triphenylphosphine-ligated tpfc compounds of both cobalt and rhodium had been published previously by my Israeli collaborator Zeev, I decided to go after Ir(III) corroles with axial py and PPh_3 ligands.

The synthesis of **1-Ir(py)$_2$** was achieved in a fashion similar to that which produced the original tma-ligated corrole complexes; however, instead of using the N-oxide as both oxidant and ligand source, I found I could simply add pyridine and allow oxygen to enter the reaction mixture at the same time. This simple procedure would form the basis of most of my future synthetic endeavors in the Ir(III) corrole arena, and in fact I have used it (with greater or lesser success depending on the ligand) to produce analogous compounds with dimethylaminopyridine (dmap), 4-cyanopyridine (cnpy), 4-methoxypyridine (meopy), 3,5-(bis)trifluoromethylpyridine (cfpy), 3,5-dichloropyridine (dcpy), and ammine axial ligands.

The triphenylphosphine-ligated Ir(III) complex **1-Ir(PPh$_3$)** could also be synthesized in this fashion, but unlike the corroles with N-donor axial ligands, the phosphine-ligated complex is only five coordinate unless large excesses of an additional axial ligand are introduced.

After I had completed the syntheses of the two iridium complexes, it was time to compare their properties with the analogous cobalt and rhodium corroles. A postdoctoral fellow in Zeev Gross' lab, Atif Mahammed, graciously provided me with the Co and Rh derivatives **1-Co(PPh$_3$)**, **1-Rh(PPh$_3$)**, **1-Co(py)$_2$**, and **1-Rh(py)$_2$**. I set out to compare: the structural parameters of the complexes; their UV-vis absorption spectra; their electrochemical properties; their affinities for a sixth ligand (in the case of the PPh$_3$-ligated compounds); and, finally, the nature of their one-electron oxidized forms.

The XRD structures of the rhodium and iridium py-ligated corroles are quite similar, whereas the cobalt complex possesses significantly foreshortened bonds between the central metal and the surrounding nitrogen atoms. Additionally, the Co(III) corrole complexes are quite labile; unlike their 4d and 5d analogues, the complexes **1-Co(PPh$_3$)** and **1-Co(py)$_2$** can be rapidly interconverted by the introduction of excess ligand. Furthermore, the preference of **1-Co(PPh$_3$)** for a five-coordinate geometry is staggeringly larger than that of the Rh(III) and Ir(III) derivatives (presumably owing to the increased van der Waals radii and electropositivity of the second and third row metals); addition of a 100,000-fold excess of triphenylphosphine to a solution of **1-Co(PPh$_3$)** causes almost no change in the observed absorption spectrum, whereas **1-Rh(PPh$_3$)** and **1-Ir(PPh$_3$)** can be converted to their six-coordinate forms by the addition of thousands and hundreds of equivalents of PPh$_3$, respectively.

In terms of molecular structure and bonding, the Co(III) complexes differ significantly from the Rh(III) and Ir(III) compounds, but in terms of electronic structure, it is the iridium that stands apart from the pack. The **1-M(py)$_2$** complexes possess similar formal $M^{IV/III}$ reduction potentials of approximately 0.7 V vs. Ag/AgCl in dcm solution, and they can all be oxidized by either the persistent organic radical oxidant (tris)(4-bromophenyl)ammoniumyl hexachloroantimonate (***t*-4bpa**) or by large excesses of iodine. By UV-vis spectroscopy, the one-electron oxidized compounds look quite similar, displaying weak transitions in the red that have been associated in the literature with corrole radical cations. However, the EPR spectrum of the iridium complex could hardly be more different from the spectra of its 3d and 4d analogues. Both the formal "Co(IV)" and "Rh(IV)" corroles (with either py or PPh_3 axial ligands) display isotropic g tensors close to the free-electron value of 2.0023. The implication in this case is that the radical is essentially organic and carbon-centered (i.e., the oxidation is ligand-centered), consistent with the UV-vis results. On the other hand, the one-electron oxidized iridium complexes **[1-Ir(py)$_2$]$^+$** and **[1-Ir(tma)$_2$]$^+$** possess extremely anisotropic g tensor components and rhombic EPR spectra; these parameters are inconsistent with a carbon-based organic radical but similar to the expected spectra for a low-spin, d^5 metal ion (for example, the low-spin Fe(III) complex **1-Fe(py)$_2$** displays this type of spectrum). Thus, I concluded that the oxidation of the Ir(III) complexes occurs on the metal instead of the ligand, and that corrole complexes of third-row metals might be able to open up new types of reactivity owing to the ability of the electron-donating macrocycles to stabilize high-valent transition metal ions. The view of the one-electron oxidized product as a pure Ir(IV) complex has been challenged by recently published theoretical work as well as unpublished XAS and DFT

studies, and these contributions will be discussed at length later in the thesis. However, the bulk of the experimental evidence, particularly the EPR spectroscopy, still suggests that the description of the one-electron oxidized products as Ir(IV) complexes is an acceptable designation.

The work summarized above was collated, edited, and interpreted over a long period of time, and finally resulted in the paper below. Many thanks are due to Kyle Lancaster, a fellow graduate student in the Gray lab, for introducing me to practical EPR spectroscopy and sparking my interest in the somewhat arcane subject of electronic structural studies. Without the early introduction of EPR spectroscopy to my arsenal (an obligatory tool in hindsight), I do not think this paper could have been written. In any case, the Inorganic Chemistry article "Structures and Reactivity Patterns of Group 9 Metallocorroles" is presented below.

Structures and Reactivity Patterns of Group 9 Metallocorroles

Abstract: Group 9 metallocorroles **1-M(PPh$_3$)** and **1-M(py)$_2$** [**M** = Co(III), Rh(III), Ir(III); **1** denotes the trianion of 5,10,15-*tris*-pentafluorophenylcorrole] have been fully characterized by structural, spectroscopic, and electrochemical methods. Crystal structure analyses reveal that average metal-N(pyrrole) bond lengths of the bis-pyridine metal(III) complexes increase from Co (1.886 Å) to Rh (1.957 Å)/Ir (1.963 Å); and the average metal-N(pyridine) bond lengths also increase from Co (1.995 Å) to Rh (2.065 Å)/Ir (2.059 Å). Ligand affinities for **1-M(PPh$_3$)** axial coordination sites increase dramatically in the order **1-Co(PPh$_3$) < 1-Rh(PPh$_3$) < 1-Ir(PPh$_3$)**. There is a surprising invariance in the **M(+/0)** reduction potentials within the five- and six-coordinate corrole series, and even between them; the average **M(+/0)** potential of **1-M(PPh$_3$)** is 0.78 V vs. Ag/AgCl in CH_2Cl_2 solution, whereas that of **1-M(py)$_2$** is 0.70 V under the same conditions. Electronic structures of one-electron-oxidized **1-M(py)$_2$** complexes have been assigned by analysis of EPR spectroscopic measurements: oxidation is corrole-centered for **1-Co(py)$_2$** (g = 2.008) and **1-Rh(py)$_2$** (g = 2.003), and metal-centered for **1-Ir(tma)$_2$** (g_{zz} = 2.489, g_{yy} = 2.010, g_{xx} = 1.884, g_{av} = 2.128) and **1-Ir(py)$_2$** (g_{zz} = 2.401, g_{yy} = 2.000, g_{xx} = 1.937, g_{av} = 2.113).

Introduction

Systematic investigations of transition metal corrole complexes have accelerated recently due to major advances in synthetic methods.[1,2,3] Many of these complexes, especially of

first-row transition metals, exhibit striking reactivity: iron(IV) derivatives remain the only non-copper catalysts for the aziridination of olefins by chloramine-T;[4] manganese(III) forms (oxo)manganese(V) during oxygenation catalysis;[5] chromium(III) mediates the aerobic oxidation of thiophenol to diphenyl disulfide;[6] and iron(I) and cobalt(I) corroles catalyze the reduction of carbon dioxide.[7] These reactivity patterns highlight the role of strong corrole σ-donation in the activation of low-valent metal centers.[8] This same electronic property, which accounts for the unusual stability of nitrido chromium(VI) and manganese(VI) complexes,[9] clearly is an important factor in metallocorrole-catalyzed processes.[10] Complexes of triarylcorroles with group 13–15 elements have been characterized as well, often with a focus on photophysical properties;[11] importantly, a gallium(III) corrole has been shown to be both an *in vivo* imaging agent and an anticancer drug candidate.[12] Second-row metallocorroles have not been investigated extensively, although there are reports of silver(III),[13] ruthenium(III),[14] and rhodium(III) derivatives, with the latter functioning as a catalyst in carbene-transfer reactions.[15] An (oxo)molybdenum(V) corrole also has been characterized.[16]

Third-row transition metal corroles are extremely rare, with fully characterized (oxo)Re(V) and Ir(III) compounds representing the only known oxidation states.[17,18] We predicted that trianionic corroles, based on their ability to stabilize numerous metals in high oxidation states,[19] would greatly stabilize iridium(III) and that these derivatives would exhibit strikingly different redox properties than iridium(III) porphyrins or organoiridium(III) complexes such as [Ir(ppy)$_3$] (ppy = 2-phenylpyridine, Figure 2-1). Indeed, Ir(III) corroles can be stabilized even by weakly donating axial ligands, whereas Ir(III) porphyrins are only stable when the metal is further coordinated by organometallic

ligands [such as in (por)Ir(CO)Cl and (por)Ir-R, where por stands for the porphyrin dianion and R = alkyl or hydride)].[20]

A stable six-coordinate (tpfc)Ir(tma)$_2$ complex (**1-Ir(tma)$_2$**, Figure 2-2) was obtained via the reaction of [Ir(cod)Cl]$_2$ with 5,10,15-*tris*-pentafluorophenylcorrole (H_3tpfc), followed by treatment with tma-N-oxide.[21] Treatment of **1-Ir(tma)$_2$** with elemental bromine in methanol yielded an octabromo complex (Br_8-tpfc)Ir(tma)$_2$ **(1b-Ir(tma)$_2$**, Figure 2-2**);** both iridium(III) derivatives were characterized by nuclear magnetic resonance (NMR) spectroscopy, mass spectrometry (MS), X-ray crystallography, UV-vis spectroscopy, and cyclic voltammetry (CV). The planar macrocyclic framework in both **1-Ir(tma)$_2$** and **1b-Ir(tma)$_2$** is quite unlike that of porphyrins, which tend to saddle or ruffle when brominated.[22] In addition, the electrochemical data suggested that the metal, rather than the macrocycle, is oxidized to Ir(IV) in both complexes, in contrast with recent findings for analogous cobalt(III) corroles.[23]

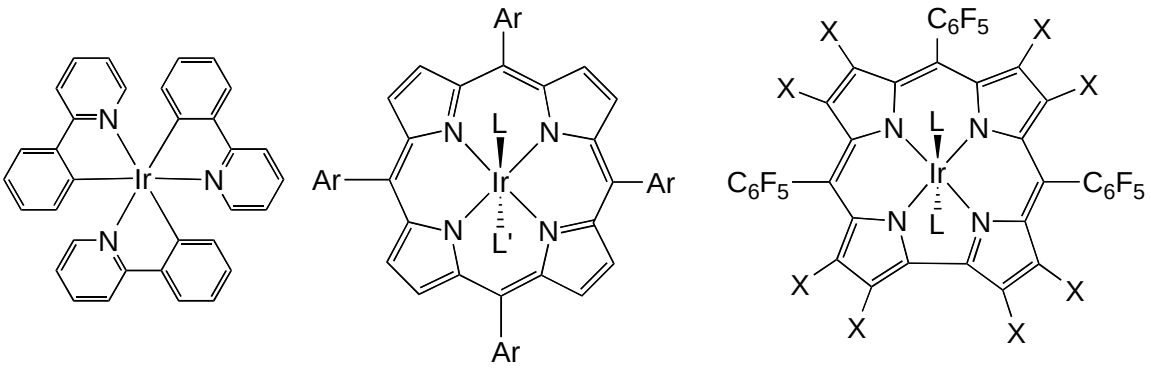

Ir(ppy)$_3$

L = CO and L' = Cl
or
L = H, alkyl (and no L')

1-Ir(tma)$_2$: X = H, L = $N(CH_3)_3$
1b-Ir(tma)$_2$: X = Br, L = $N(CH_3)_3$

Figure 2-1: Complexes of 2-phenylpyridine, porphyrins, and corroles with iridium(III)

Here we report the synthesis and characterization of corroles **1-Ir(py)$_2$** and **1-Ir(PPh$_3$)**, whose properties are compared with those of isostructural cobalt(III) and rhodium(III) analogues **1-Co(py)$_2$**, **1-Rh(py)$_2$**, **1-Co(PPh$_3$)**, and **1-Rh(PPh$_3$)** (Figure 2-2). Each set, **1-M(py)$_2$** or **1-M(PPh$_3$)**, represents a rare example of an entire transition metal group with the same oxidation state and coordination number, another being the Group 8 (por)M-CO series.[24] Our research has focused on the substitutional lability of Group 9 metallocorroles and the sites of oxidation reactions, as both change markedly within the group. We have found that: Co(III) corroles are far more substitutionally labile than analogous Rh(III) or Ir(III) derivatives; the affinity of five-coordinate **1-M(PPh$_3$)** for a sixth ligand increases dramatically down the row; and oxidation of **1-M(py)$_2$** occurs primarily on the metal rather than on the macrocyclic ligand only in the case of iridium ($Ir^{III/IV}$). We report extensive electronic absorption, electrochemical, and EPR data that support these conclusions.

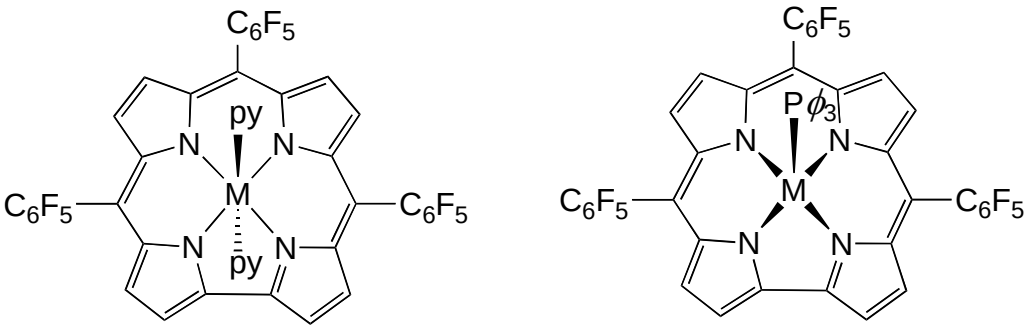

1-Ir(py)$_2$: M = iridium(III)
1-Rh(py)$_2$: M = rhodium(III)
1-Co(py)$_2$: M = cobalt(III)

1-Ir(PPh$_3$): M = iridium(III)
1-Rh(PPh$_3$): M = rhodium(III)
1-Co(PPh$_3$): M = cobalt(III)

Figure 2-2: Axially ligated metal(III) corroles (py = pyridine)

Experimental Section

Materials. Silica gel for column chromatography (Silica Gel 60, 63-200 micron mesh) was obtained from EMD Chemicals, as were all solvents (THF, toluene, CH_2Cl_2, hexanes, and methanol). Most starting materials for syntheses were from Sigma-Aldrich and used without further purification. Exceptions are pyrrole and pentafluorobenzaldehyde, which were both purified by vacuum distillation before use. Tetrabutylammonium hexafluorophosphate, which was used as a supporting electrolyte in the CV experiments, was also from Sigma-Aldrich and used without further purification. Electrodes for CV were obtained from CH Instruments.

Syntheses. The synthesis of 5,10,15-*tris*-pentafluorophenylcorrole (the H_3tpfc ligand) was accomplished by a simplified version of the standard procedure outlined in reference 1c.[25] The cobalt(III) and rhodium(III) corroles were available from previous studies.[15,26] Compounds **1-Ir(tma)$_2$** and **1b-Ir(tma)$_2$** have only been reported in a previous communication,[18] hence their syntheses are summarized below along with those of the new corroles.

5,10,15-*tris*-pentafluorophenylcorrolato-iridium(III) *bis*-trimethylamine, 1-Ir(tma)$_2$. H_3tpfc (80 mg), $[Ir(cod)Cl]_2$ (335 mg), and K_2CO_3 (140 mg) were dissolved/suspended in 150 mL of degassed THF, and the mixture was heated at reflux under argon for 90 min (until corrole fluorescence was negligible to the eye upon long-wavelength irradiation with a hand-held lamp). Tma N-oxide (110 mg) was added, and the solution was allowed to slowly cool to room temperature while open to the laboratory atmosphere. Column chromatography of the black mixture (silica, 4:1 hexanes:CH_2Cl_2) provided an auburn

solution, from which purple crystals of (tpfc)Ir(III)$(tma)_2$ (30 mg, 27% yield) could be grown by slow evaporation. ^{1}H NMR ($CDCl_3$): δ 8.90 (d, 2H, J = 4.2), 8.50 (d, 2H, J = 5.1), 8.38 (d, 2H, J = 4.5), 8.09 (d, 2H, J = 4.2), -2.95 (s, 18H). ^{19}F NMR ($CDCl_3$): δ -138.38 (m, 6F), -154.89 (m, 3F), -163.27 (m, 6F). MS (ESI): 1105.1 ([M^+]), 1046.0 ([M^+-tma]), 986.5 ([M^+-2tma]). UV-vis (CH_2Cl_2, nm, ε x 10^{-3} $M^{-1}cm^{-1}$): 388 (47), 412 (56), 572 (14), 640 (5.3)

2,3,7,8,12,13,17,18-octabromo-5,10,15-*tris*-pentafluorophenylcorrolato-iridium(III) *bis*-trimethylamine, 1b-Ir(tma)$_2$. Compound 1-Ir$(tma)_2$ (15 mg) and Br_2 (70 μL) were dissolved in 20 mL MeOH and stirred overnight. Column chromatography (silica, 4:1 hexanes:CH_2Cl_2) of the red mixture provided a ruddy solution from which purple crystals of (Br_8-tpfc)Ir(III)$(tma)_2$ (15 mg, 63% yield) could be grown by addition of methanol followed by slow evaporation. ^{1}H NMR ($CDCl_3$): δ -2.60 (s, 18H). ^{19}F NMR ($CDCl_3$): δ -137.78 (d/d, 2F, ^{3}J = 35.1, ^{4}J = 18.3), -138.54 (d/d, 4F, ^{3}J = 33.9, ^{4}J = 17.1), -152.89 (m, 3F), -163.38 (m, 4F), -163.70 (m, 2F). MS (ESI): 1616.4 ([M^+-2tma]). UV-vis (CH_2Cl_2, nm, ε x 10^{-3} $M^{-1}cm^{-1}$): 404 (61), 424 (70), 580 (16), 654 (7.3)

5,10,15-*tris*-pentafluorophenylcorrolato-iridium(III) *bis*-pyridine, 1-Ir(py)$_2$. H_3tpfc (40 mg), [Ir(cod)Cl]$_2$ (170 mg), and K_2CO_3 (70 mg) were dissolved/suspended in 75 mL of degassed THF, and the mixture was heated at reflux under argon for 90 min. Pyridine (1 mL) was added, and the solution was allowed to slowly cool to room temperature while open to the laboratory atmosphere. Column chromatography of the forest green mixture (silica, 4:1 hexanes:CH_2Cl_2 followed by 3:2 hexanes:CH_2Cl_2) afforded a bright green solution, from which thin, green crystals of (tpfc)Ir(III)$(py)_2$ (26 mg, 50% yield)

could be grown by addition of methanol followed by slow evaporation. ^{1}H NMR ($CDCl_3$): δ 8.84 (d, 2H, J = 4.5), 8.53 (d, 2H, J = 4.8), 8.32 (d, 2H, J = 4.8), 8.17 (d, 2H, J = 4.5), 6.21 (t, 2H, J = 7.8), 5.19 (t, 4H, J = 7.0), 1.72 (d, 4H, J = 5.1). ^{19}F NMR ($CDCl_3$): δ -138.68 (m, 6F), -154.84 (t, 2F, J = 22.2), -155.20 (t, 1F, J = 22.2), -163.28 (m, 4F), -163.65 (m, 2F). MS (ESI): 1144.1 ([M^+]). UV-vis (CH_2Cl_2, nm, ε x 10^{-3} $M^{-1}cm^{-1}$): 390 (28), 412 (43), 582 (12), 619 (6.5)

5,10,15-*tris*-pentafluorophenylcorrolato-iridium(III) triphenylphosphine, 1-Ir(PPh_3). H_3tpfc (40 mg), $[Ir(cod)Cl]_2$ (170 mg), and K_2CO_3 (70 mg) were dissolved/suspended in 75 mL of degassed THF, and the mixture was heated at reflux under argon for 90 min. Triphenylphosphine (260 mg dissolved in 5 mL THF) was added, and the solution was heated at reflux for another half hour under laboratory atmosphere before being allowed to cool to room temperature. Column chromatography of the deep green mixture (silica, 3:1 hexanes:CH_2Cl_2) afforded a bright red-orange solution, which could be evaporated to give (tpfc)Ir(III)(PPh_3) (30 mg, 64% yield) as a ruby-colored solid. ^{1}H NMR ($CDCl_3$): δ 8.67 (d, 2H, J = 4.5), 8.36 (d, 2H, J = 5.1), 8.18 (d, 2H, J = 5.1), 8.00 (d, 2H, J = 4.5), 6.98 (t, 3H, J = 7.2), 6.69 (t, 6H, J = 6.9), 4.52 (d/d, 6H, ^{3}J = 19.5, ^{4}J = 3.6). ^{19}F NMR ($CDCl_3$): δ -137.44 (m, 6F), -154.05 (m, 3F), -162.54 (m, 3F). MS (ESI): 1248.1 ([M^+]). UV-vis (CH_2Cl_2, nm, ε x 10^{-3} $M^{-1}cm^{-1}$): 398 (66), 554 (8.8), 588 (6.7)

Nuclear Magnetic Resonance Spectroscopy. ^{1}H and ^{19}F NMR data were obtained on $CDCl_3$ solutions of each compound at room temperature using a Varian Mercury 300

MHz NMR spectrometer. ^{1}H chemical shifts are reported relative to solvent peaks and ^{19}F chemical shifts are reported relative to a saved, external $CFCl_3$ standard.

Mass Spectrometry. Measurements were made on CH_3OH solutions of each compound by electrospray ionization into a Thermofinnigan LCQ ion trap mass spectrometer.

X-ray Crystallography. Concentrated CH_2Cl_2/CH_3OH solutions of corroles 1-Ir(tma)$_2$, 1b-Ir(tma)$_2$, and 1- Ir(py)$_2$ were allowed to undergo slow evaporation from scintillation vials. The resultant crystals were mounted on a glass fiber using Paratone oil and then placed on a Bruker Kappa Apex II diffractometer under a nitrogen stream at 100 K. The SHELXS-97 program was used to solve the structures.

Cyclic Voltammetry. CV measurements were made with a WaveNow USB Potentiostat/Galvanostat (Pine Research Instrumentation) using Pine AfterMath Data Organizer software. A three electrode system consisting of a platinum wire working electrode, a platinum wire counter electrode, and an Ag/AgCl reference electrode, was employed. The CV measurements were made using dichloromethane solutions, 0.1 M in tetrabutylammonium perchlorate (TBAP, Fluka, recrystallized twice from absolute ethanol) and 10^{-3} M substrate under an argon atmosphere at ambient temperature. The scan rate was 0.1 V/s and the $E_{1/2}$ value for oxidation of ferrocene under these conditions was 0.55 V.

UV-visible spectroelectrochemical measurements were made on dichloromethane solutions, 0.5 M in TBAP and 0.1–0.3 mM in substrate with an optically transparent platinum thin-layer electrode working electrode, a platinum wire counter electrode, and

an Ag/AgCl reference electrode under an argon atmosphere at ambient temperature. Potentials were applied with a WaveNow USB Potentiostat/Galvanostat. Time-resolved UV-visible spectra were recorded with a Hewlett-Packard Model 8453 diode array rapid-scanning spectrophotometer.

Electron Paramagnetic Resonance Spectroscopy. Solutions for EPR were prepared by adding 50 μL of a 10 mM CH_2Cl_2 solution of iodine to 100 uL of a 1 mM CH_2Cl_2 solution of the corrole being examined, ensuring complete one-electron oxidation of the substrate. In order to rule out side reactions with iodine, sub-stoichiometric amounts of the radical cation *tris*(4-bromophenyl)aminium hexachloroantimonate (***t*-4bpa**) also were employed for oxidations. Spectra taken of the products obtained from reactions with both oxidants were virtually identical. EPR spectroscopy was performed using a Bruker EMX Biospin instrument, with a Gunn diode microwave source. Solutions were pre-cooled by rapid freezing in liquid nitrogen; spectra of samples at 20 K were obtained using liquid helium as a coolant. The SPINCOUNT package was used to simulate EPR parameters.

UV-vis Absorption Spectroscopy. Absorption spectral measurements were made on solutions of each compound in CH_2Cl_2, using a Hewlett-Packard 8452A Diode Array Spectrophotometer. Extinction coefficients were calculated from measurements on corroles at variable concentrations in CH_2Cl_2 solutions. UV-vis spectroscopic titrations were performed by stepwise addition of small aliquots of CH_2Cl_2 solutions of ***t*-4bpa** to CH_2Cl_2 solutions of each corrole. The ***t*-4bpa** oxidant was employed rather than iodine owing to overlapping absorptions due to excess reagent in the latter case.

Results and Discussion

Iridium(III) corroles. The insertion of the metal ion into the free base corrole H_3(tpfc) was achieved via heating with $[Ir(cod)Cl]_2$ and K_2CO_3 in THF under an inert atmosphere. This procedure was followed by addition of pyridine or triphenylphosphine and opening the reaction mixture to the laboratory atmosphere to effect aerobic oxidation.[27] Owing to their low-spin d^6 electronic configurations, iridium(III) corroles display highly resolved NMR spectra that are characteristic of diamagnetic complexes,[28] as shown in Figure 2-3 (upper) for **1-Ir(py)$_2$**. The ^{1}H NMR spectra reveal four β-pyrrole CH proton resonances as doublets with *J* coupling constants of about 4.5 Hz at 8–9 ppm and axial ligand resonances at high field attributable to the diamagnetic ring current of the aromatic corrole. The **1-Ir(py)$_2$** pyridine proton resonances are more shifted than those of PPh_3 in **1-Ir(PPh$_3$)** (both relative to their positions in the absence of a metal center) due to the proximity of py protons to the corrole ring. The coordination number [six for the bis-pyridine complex **1-Ir(py)$_2$** and five for the triphenylphosphine complex **1-Ir(PPh$_3$)**] can be deduced from ^{1}H NMR spectra via integration of the relevant proton resonances. The same information can also be extracted from the ^{19}F NMR spectra (Figure 2-3, lower), since the C_{2v} symmetry of **1-Ir(py)$_2$** requires equivalence of above- and below-plane *ortho*- and *meta*-fluorine atoms on each C_6F_5 ring.

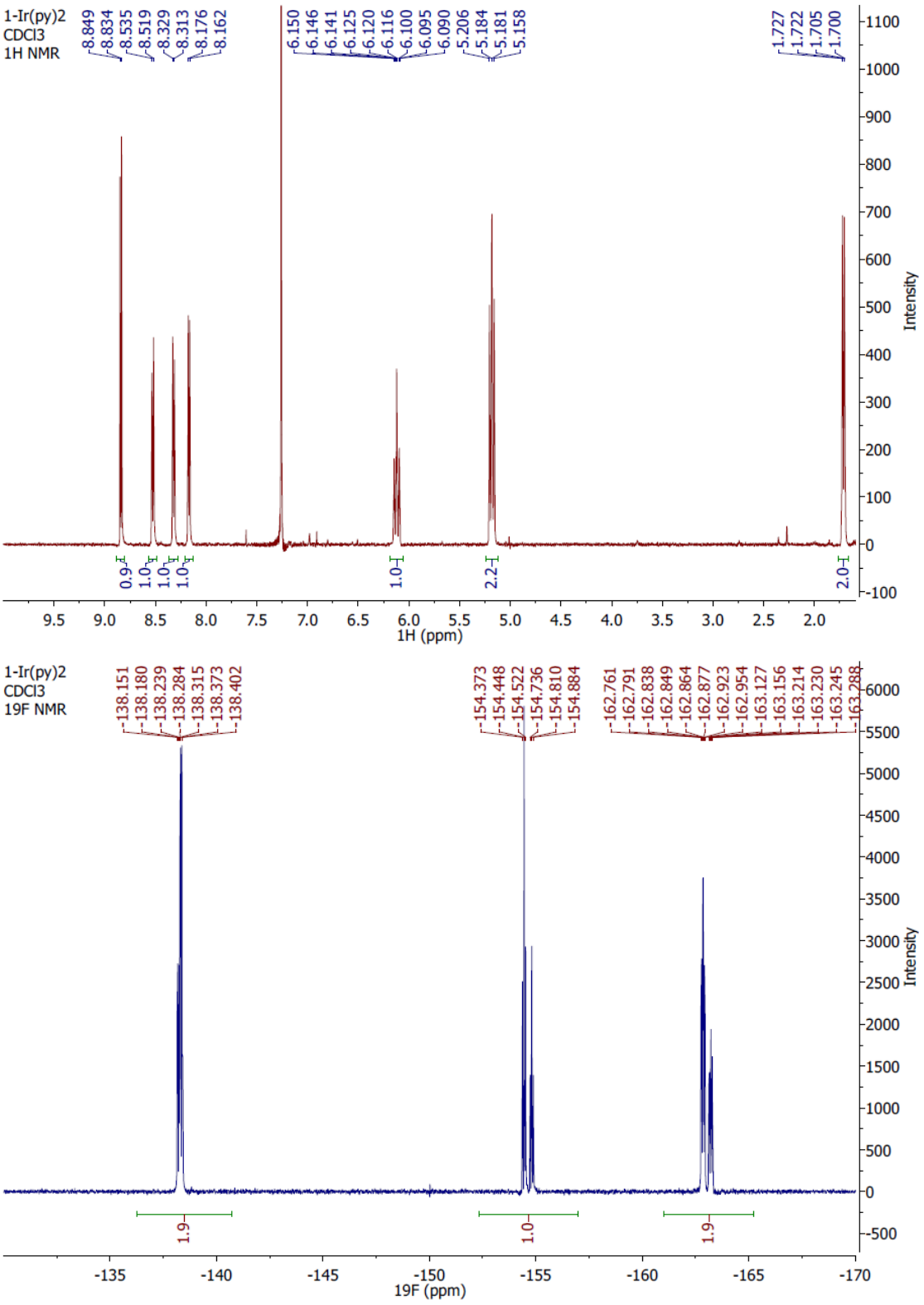

Figure 2-3: ^{1}H (top) and ^{19}F (bottom) NMR spectra of **1-Ir(py)$_2$**

The electronic absorption spectra of six-coordinate metal(III) corroles are shown in Figure 2-4. The spectra of **1-Co(py)$_2$** and **1-Rh(py)$_2$** are similar, each with one major Soret band and Q bands near 580 and 600 nm, whereas the spectrum of **1-Ir(py)$_2$** exhibits highly structured Soret absorption with Q bands that are red-shifted by about 20 nm compared to those of the 3d and 4d analogues. We emphasize that **1-Co(py)$_2$** is in equilibrium with the (mono)pyridine complex **1-Co(py)** in CH_2Cl_2 solution [which is not the case for **1-Rh(py)$_2$** or **1-Ir(py)$_2$**].[26b] The spectrum of **1-Co(py)$_2$** in 5% pyridine (where only the (bis)ligated form exists in solution) is in Supporting Information. As the main components of the electronic spectra are attributable to corrole-based π-π^* transitions, the differences likely reflect increased mixing with MLCT in the order Co < Rh < Ir. Red-shifted Q bands also are exhibited by five-coordinate **1-Ir(PPh$_3$)**, while the Soret bands differ markedly, as follows: **1-Co(PPh$_3$)** has a highly split system, **1-Rh(PPh$_3$)** displays less splitting but is red-shifted, and **1-Ir(PPh$_3$)** exhibits a single, relatively sharp Soret band.

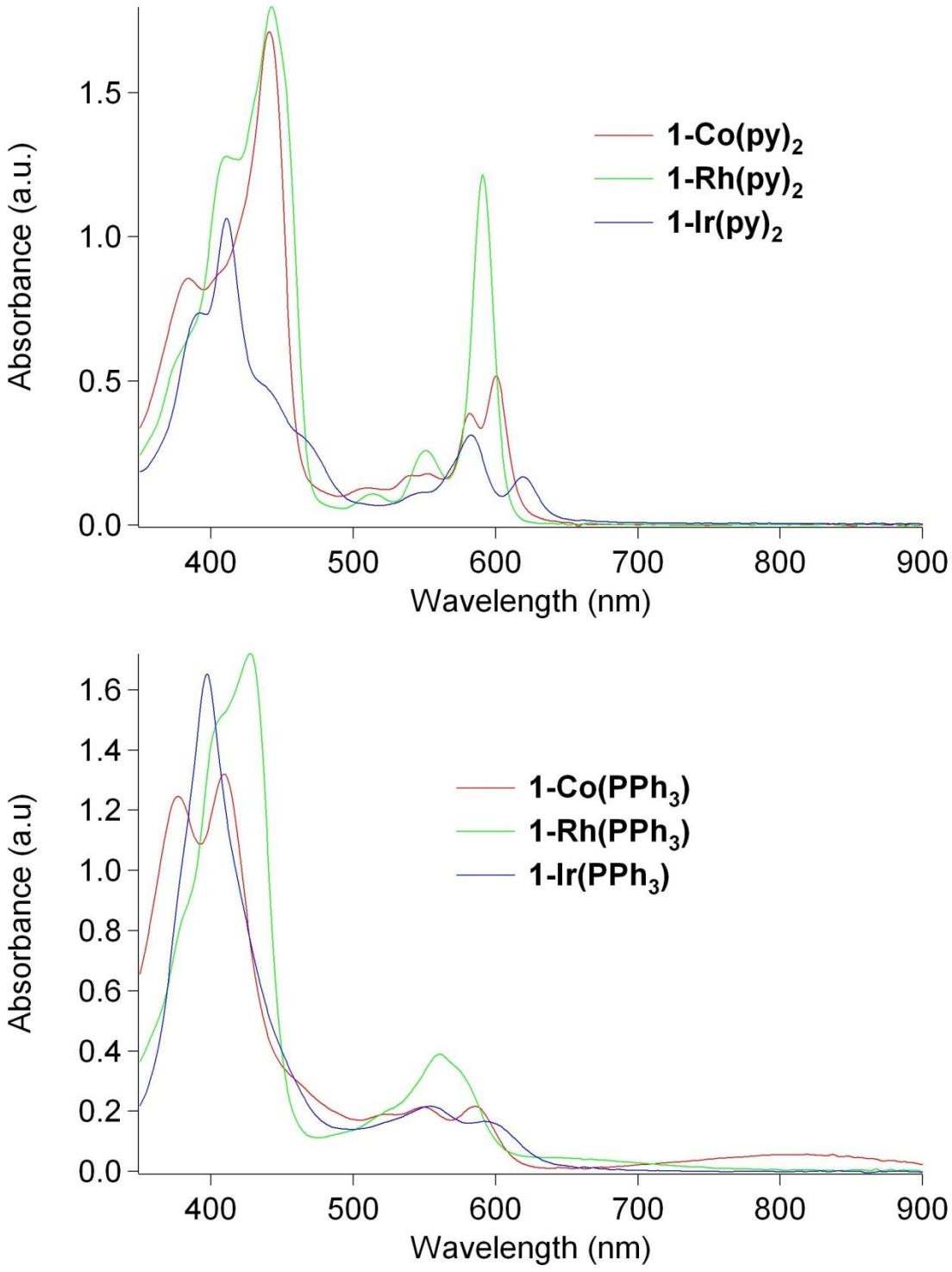

Figure 2-4: Electronic absorption spectra of six-coordinate (bis)pyridine metal(III) corroles (top) and five-coordinate PPh_3-ligated metal(III) corroles (bottom); 2.5 μM in CH_2Cl_2 solution

	M-N(corrole)	M-N(axial)	Reference
1-Co(py)$_2$	1.873(4)–1.900(4)	1.994(4)–1.995(4)	26b
1-Rh(py)$_2$	1.938(5)–1.976(5)	2.060(5)–2.071(5)	15
1-Ir(py)$_2$	1.947(2)–1.979(2)	2.052(2)–2.066(2)	This work
1-Ir(tma)$_2$	1.940(3)–1.981(3)	2.184(3)–2.186(3)	18
1b-Ir(tma)$_2$	1.959(2)–1.989(2)	2.186(2)–2.192(2)	18

Table 2-1: Metal-nitrogen bond lengths (Å) in **1-Co(py)$_2$**, **1-Rh(py)$_2$**, **1-Ir(py)$_2$**, **1-Ir(tma)$_2$**, and **1b-Ir(tma)$_2$**

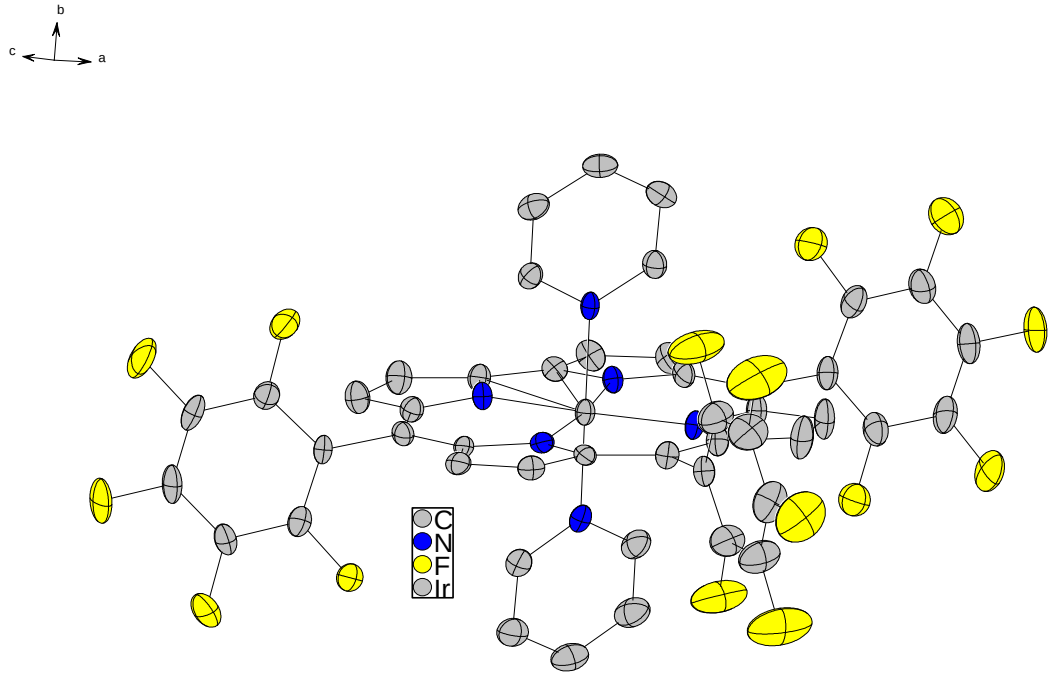

Figure 2-5: Structure of **1-Ir(py)$_2$** (H atoms omitted)

Substitution and addition reactions. Previous investigations have revealed that **1-Co(PPh$_3$)** and **1-Rh(PPh$_3$)** react differently with pyridine: both ligand substitution and addition to Co(III) yield **1-Co(py)$_2$**, but Rh(III) undergoes only addition to give **1-Rh(PPh$_3$)(py)**.[26b,29] The reactivity of **1-Ir(PPh$_3$)** is similar to that of Rh(III), i.e., addition of pyridine produces a mixed-ligand complex (see Supporting Information). Additional confirmation of the substitutional lability of the Co(III) corrole is the observation (Figure 2-6a) that addition of PPh_3 to **1-Co(py)$_2$** rapidly yields **1-Co(PPh$_3$)** [addition of excess pyridine regenerates the bis-pyridine complex; the spectrum changes slightly due to the absence of 5-coordinate **1-Co(py)** under these conditions]. Complementary information was obtained by examination of spectral changes upon the addition of PPh_3 to five-coordinate metallocorroles. While addition of a 100,000-fold excess of triphenylphosphine produced only minor changes in the spectrum of **1-Co(PPh$_3$)** (see Supporting Information), the spectra of **1-Rh(PPh$_3$)** (Figure 2-6b) and **1-Ir(PPh$_3$)** (Figure 2-6c) changed completely after the addition of 6300 and 350 equivalents, respectively. The similarity of the visible spectra obtained upon addition of triphenylphosphine to **1-Rh(PPh$_3$)** and **1-Ir(PPh$_3$)** to those of **1-Rh(py)$_2$** and **1-Ir(py)$_2$** suggests that the products are six-coordinate (bis)triphenylphosphine species, **1-Rh(PPh$_3$)$_2$** and **1-Ir(PPh$_3$)$_2$**. While many corrole-chelated metal(III) ions possess surprisingly low affinities for a sixth ligand,[26b,30,31] our work demonstrates that this property is not as pronounced for 4d and especially for 5d metals.

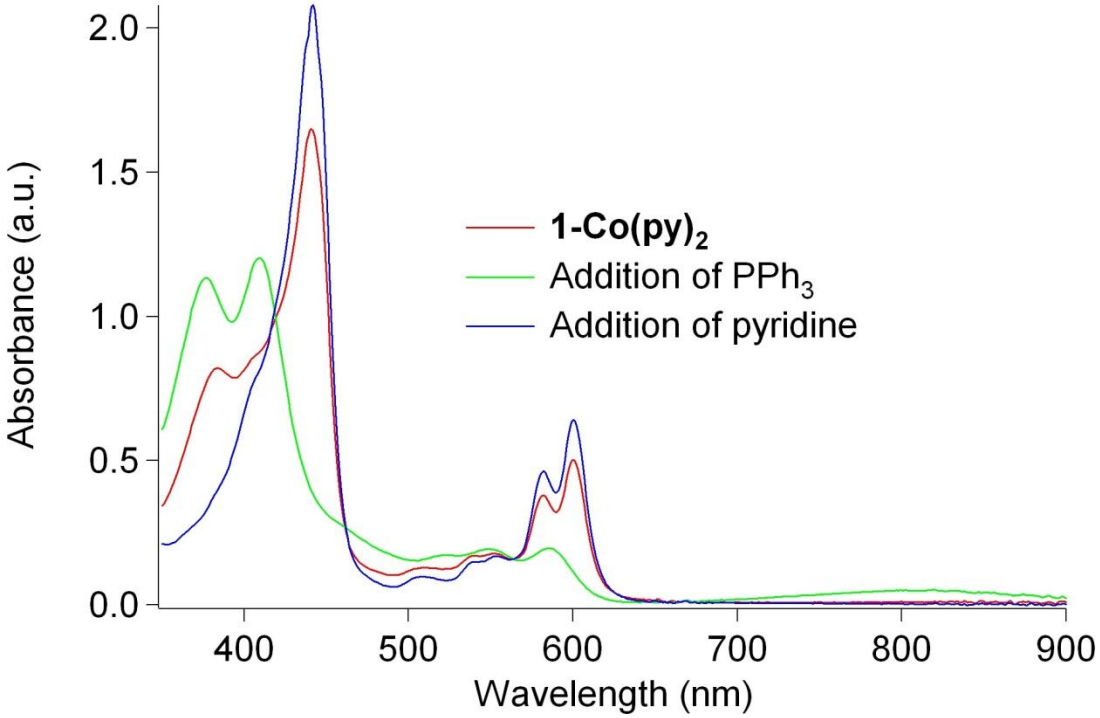
Absorbance (a.u.)
2.0
1.5
1.0
0.5
0.0
400
500
600
700
800
900
Wavelength (nm)
1-Co(py)2
Addition of PPh3
Addition of pyridine

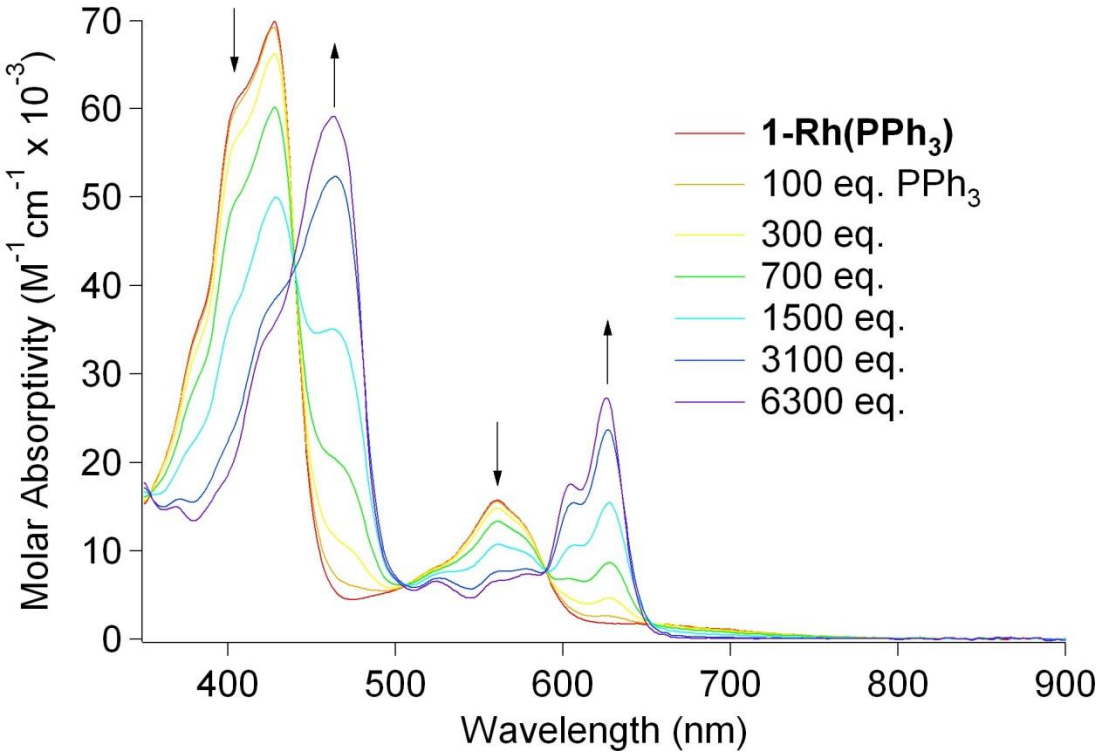
Molar Absorptivity (M-1cm-1 x 10-3)
70
60
50
40
30
20
10
0
400
500
600
700
800
900
Wavelength (nm)
1-Rh(PPh3)
100 eq. PPh3
300 eq.
700 eq.
1500 eq.
3100 eq.
6300 eq.

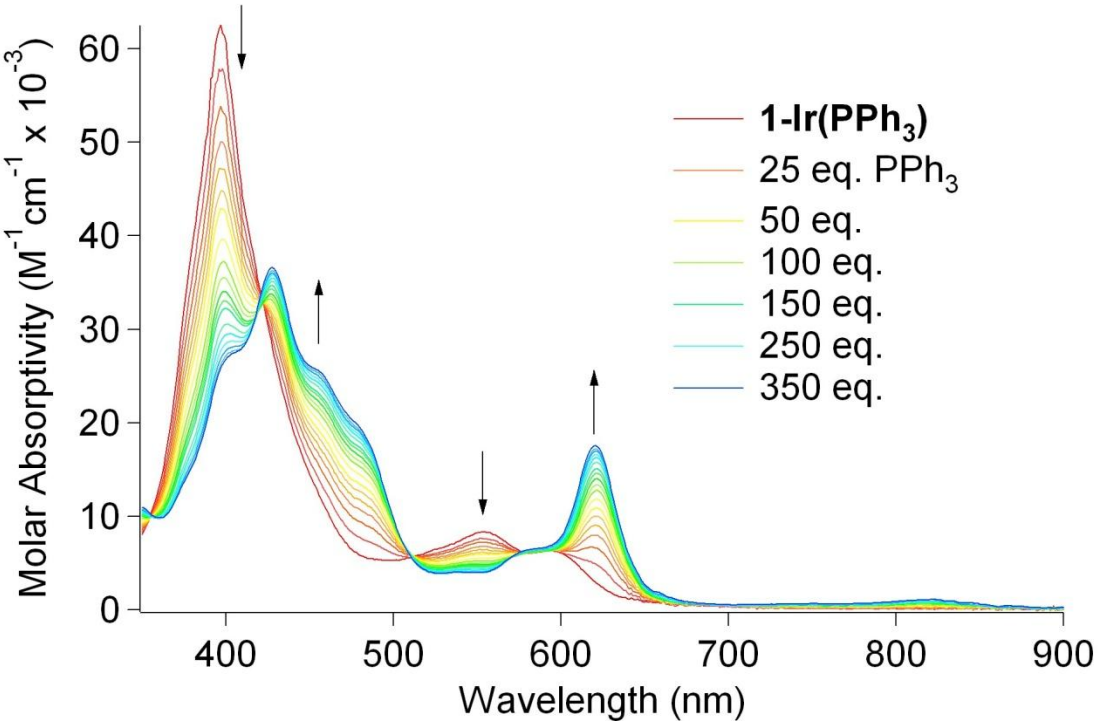

Figure 2-6: Electronic absorption spectra of metal(III) corroles in CH_2Cl_2 solution demonstrate: (a, top), reversible transformations between **1-Co(py)$_2$** and **1-Co(PPh$_3$)** upon addition of PPh_3 and pyridine; (b, middle), formation of **1-Rh(PPh$_3$)$_2$**; (c, bottom), formation of **1-Ir(PPh$_3$)$_2$.** Only a representative selection of the many individual traces (25 to 350 eq. ligand) that are shown in the bottom panel are specifically identified

Electrochemistry. Our earlier work focused on the differences between the β-pyrrole-unsubstituted complex **1-Ir(tma)$_2$** and its fully brominated analogue, **1b-Ir(tma)$_2$.** The latter displays one oxidation (at 1.19 V vs. SCE) and one reduction (at -1.21 V vs. SCE) within the solvent potential window of CH_2Cl_2, while two reversible oxidations (at 0.66 and 1.28 V vs. SCE) were observed for the former.[18] The current emphasis is on the **M(+/0)** reduction potential of each of the complexes, because it should correspond to either a metal-centered (M^{III}/M^{IV}, where M = Co, Rh, or Ir) or ligand-centered (tpfc/tpfc$^{+\cdot}$) process. The CVs of all complexes are shown in Figure 2-7; and Table 2-2 lists the corresponding reduction potentials. The results reveal that six-coordinate **1-M(py)$_2$** complexes are oxidized at lower potentials than five-coordinate **1-M(PPh$_3$)** and

that the differences become larger in the order Ir < Rh < Co. It is surprising that there are only very small differences in reduction potentials for the two series: 0.70 ± 0.03 for **1-M(py)$_2$** and 0.78 ± 0.06 for **1-M(PPh$_3$)**. Very large potential shifts would be expected for metal-based processes ($M^{III/IV}$), as documented by the finding that $Rh^{III/IV}$ reduction potentials are 0.2 to 0.3 V more positive than $Ir^{III/IV}$ potentials in cyclometalated complexes.[32] A caveat is that the central metal ion should have some effect on the potential even in the case of macrocycle-centered oxidation, as observed previously for both corroles and porphyrins.[33,34]

1-M(PPh$_3$)$_2$	$E_{1/2}$	**1-M(py)$_2$**	$E_{1/2}$
M= Co	0.83	M= Co	0.67
M = Rh	0.79	M = Rh	0.72
M = Ir	0.72	M = Ir	0.71

Table 2-2: Reduction potentials (CH_2Cl_2, TBAP, V vs. Ag/AgCl) for Group 9 metal(III) corroles. Under virtually identical conditions, $E_{1/2}$ for ferrocene is 0.55 V; and iodine has E_{pa} of 0.89 V and E_{pc} of 0.39 V.

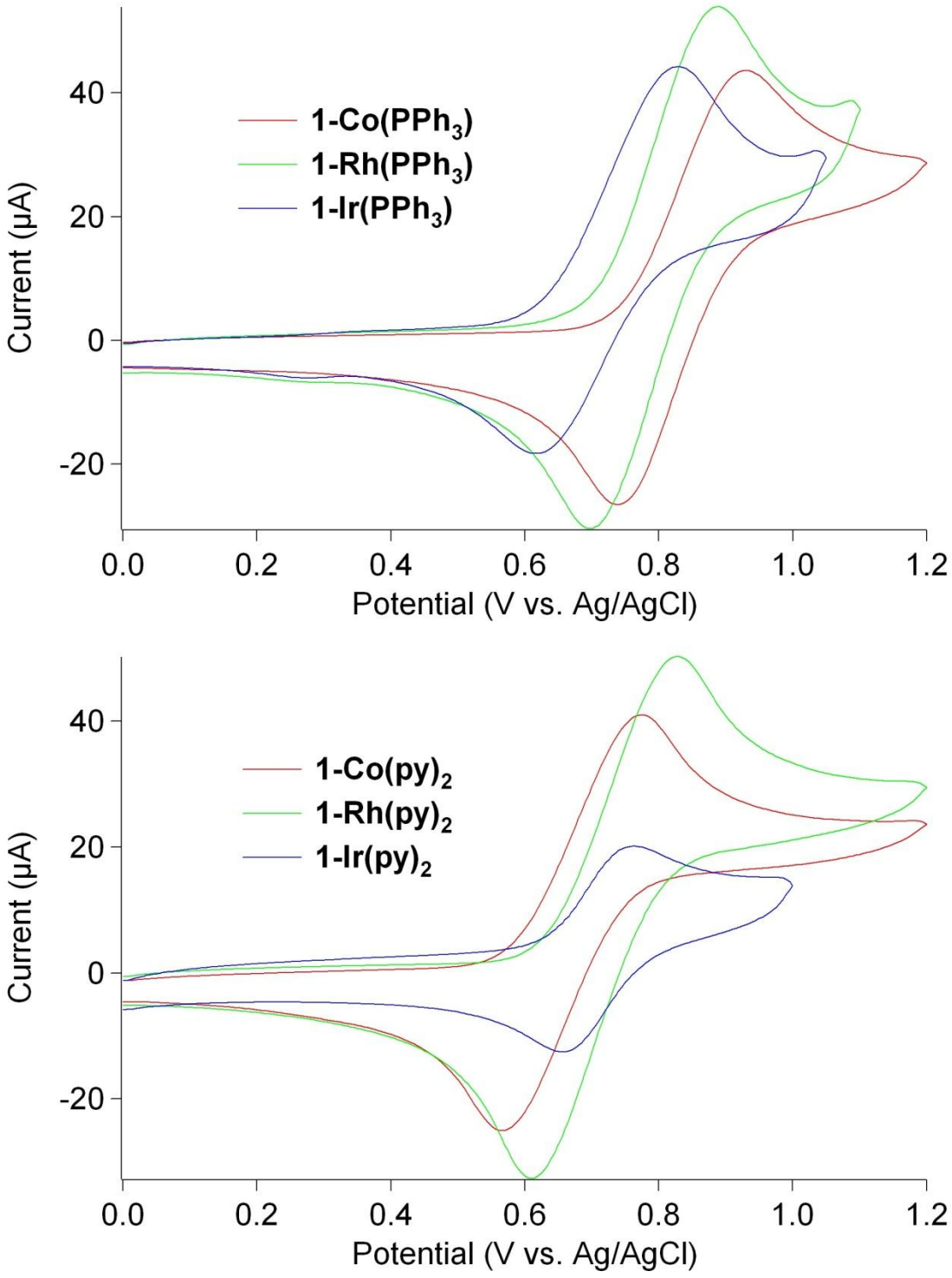

Figure 2-7: CV traces of **1-M(PPh$_3$)** (top) and **1-M(py)$_2$** (bottom), in CH_2Cl_2 solution

Electronic structures of one-electron-oxidized metallo(III)corroles. Changes in electronic spectra upon M(III) corrole oxidation can be used as a tool for analyzing whether an electron is removed primarily from a metal or ligand orbital. One-electron oxidation of 1-Co(PPh_3) or 1-Rh(PPh_3) by ***t*-4bpa** (Figure 2-8) was marked by substantial intensity reductions of the M(III) Soret and Q bands and formation of a broad absorption system at 690 ($\varepsilon = 4000\ M^{-1}cm^{-1}$) for cobalt and 710 nm ($\varepsilon = 2300\ M^{-1}cm^{-1}$) for rhodium. These long-wavelength absorption features, which appear at 673 nm ($\varepsilon = 3000\ M^{-1}cm^{-1}$ for Co and $4100\ M^{-1}cm^{-1}$ for Rh) in the spectra of chemically oxidized 1-Co($py)_2$ and 1-Rh($py)_2$ complexes (Figure 2-9), represent signature spectroscopic features for corrole-centered oxidations.

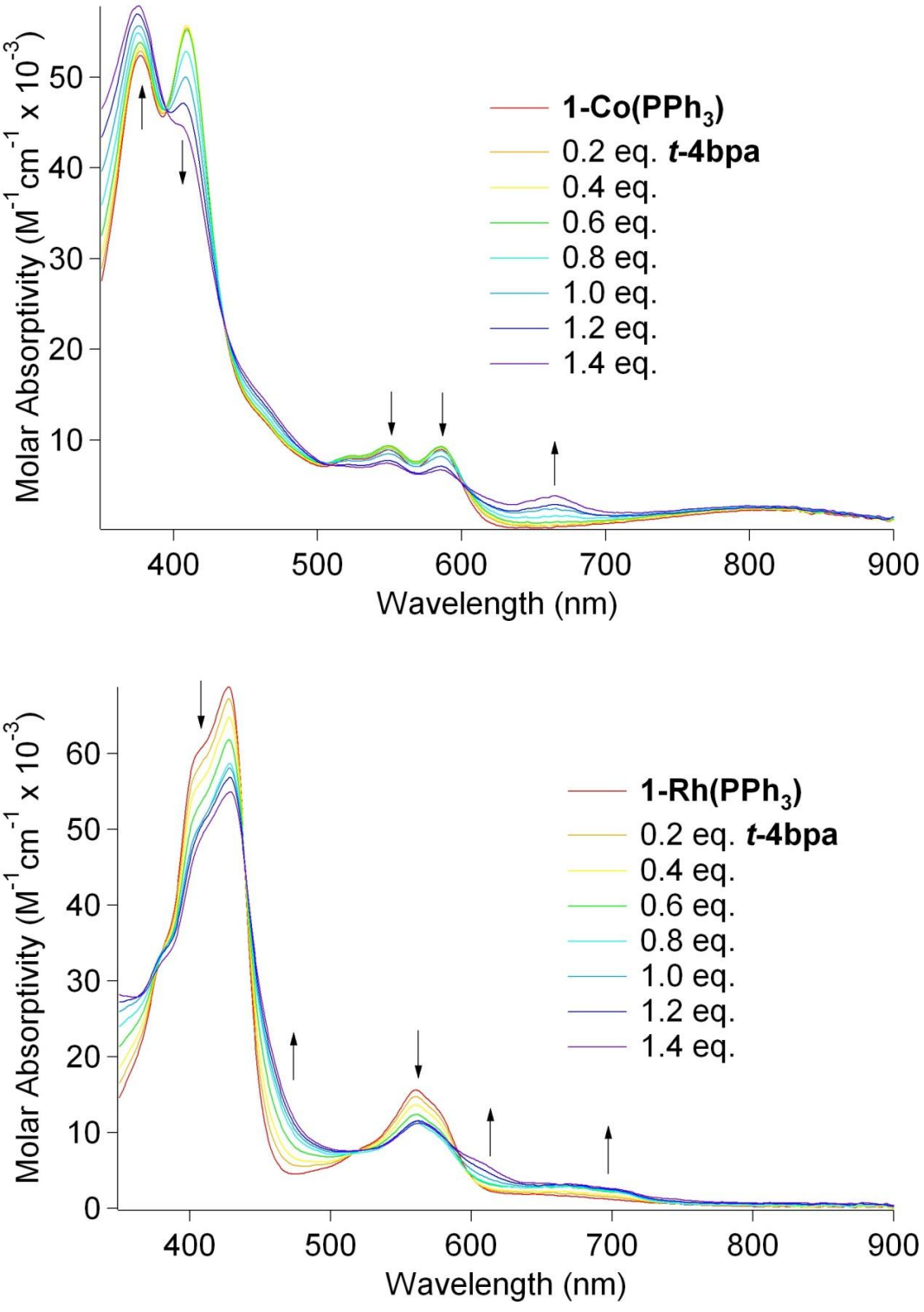

Figure 2-8: Absorption spectral changes accompanying oxidation of **1-Co(PPh)$_3$** (top) and **1-Rh(PPh)$_3$** (bottom) by ***t*-4bpa** in CH_2Cl_2 solution

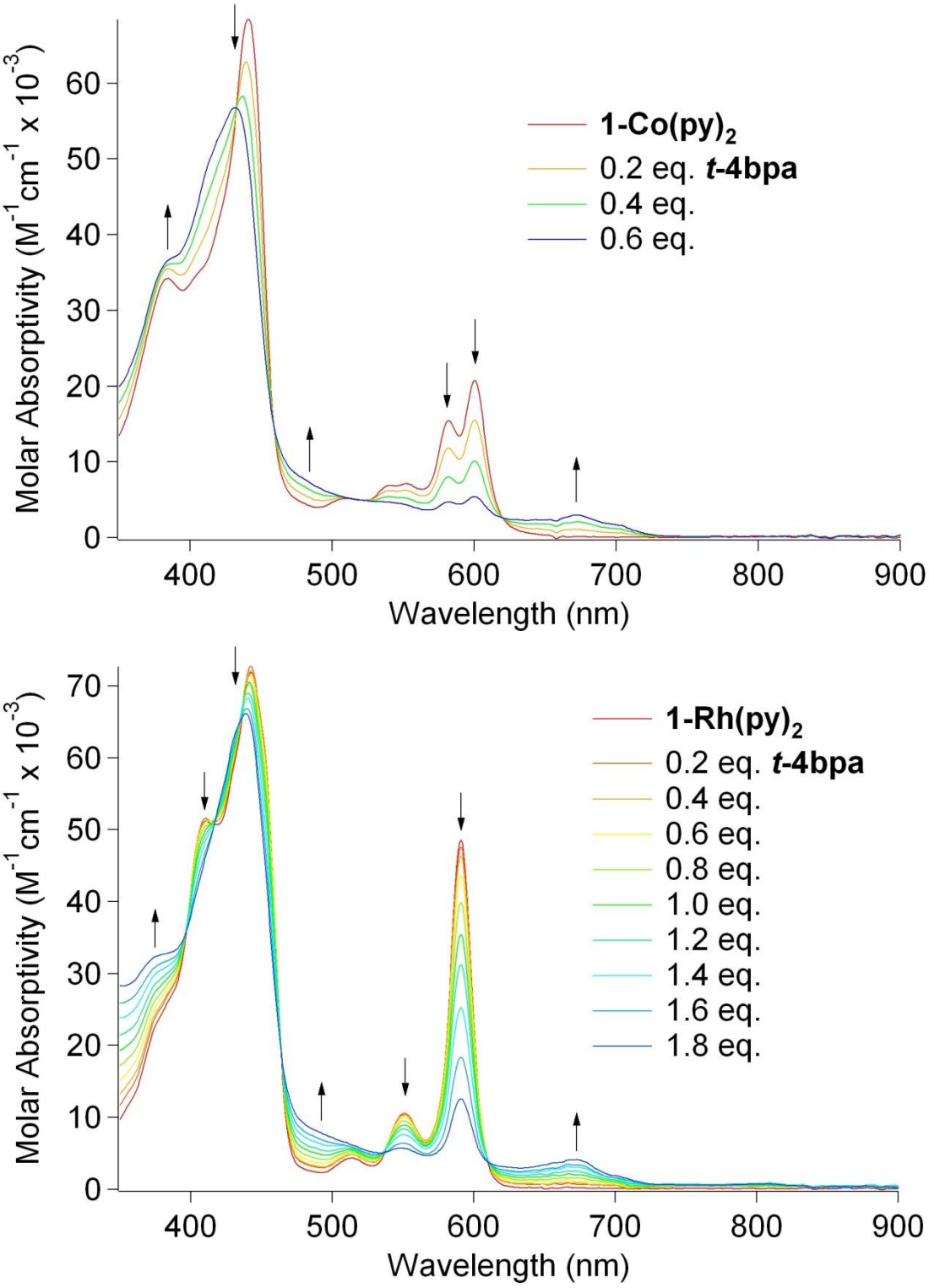

Figure 2-9: Absorption spectral changes accompanying oxidation of **1-Co(py)$_2$** (top) and **1-Rh(py)$_2$** (bottom) by ***t*-4bpa** in CH_2Cl_2 solutions. Reaction with the Co(III) complex was terminated after addition of 0.6 equivalents, owing to product instability.[26b]

Absorption spectral changes upon oxidation of iridium(III) corroles are substantially different from those of 3d and 4d analogues. Oxidations of **1-Ir(PPh$_3$)**, **1-Ir(py)$_2$**, and **1-Ir(tma)$_2$** by ***t*-4bpa** in CH_2Cl_2 were performed, and their progress was tracked by UV-visible spectroscopy (Figure 2-10). In the case of the five-coordinate complex **1-Ir(PPh$_3$)**, oxidation causes a significant reduction in the intensity of the Soret system, accompanied by broadening, and the Q-bands are slightly red-shifted. For each of the six-coordinate complexes **1-Ir(py)$_2$** and **1-Ir(tma)$_2$**, the Soret band blue shifts over 30 nm to 366 nm and the Q-bands all but vanish. A weak absorption appears at 695 nm (ε = 3000 $M^{-1}cm^{-1}$) in the spectrum of **1-Ir(PPh$_3$)**; and a similar system is centered at 685 nm (ε = 2600 $M^{-1}cm^{-1}$) in the spectra of the six-coordinate complexes; these features are red-shifted from the 673 nm band observed upon oxidation of either **1-Co(py)$_2$** or **1-Rh(py)$_2$**, suggesting that the site of oxidation is different for Ir(III). As it is well established that substantial blue shifts of Soret bands accompany metal-centered oxidations[1] of metallocorroles,[5b,35] an Ir(IV) oxidation state is indicated for each of the one-electron-oxidized Ir(III) complexes.

[1] Note that a 32 nm blue shift in the Soret peak occurs upon oxidation of **[1-Cr^{IV}(O)]$^-$** to **[1-Cr^{V}(O)]** (see reference 35).

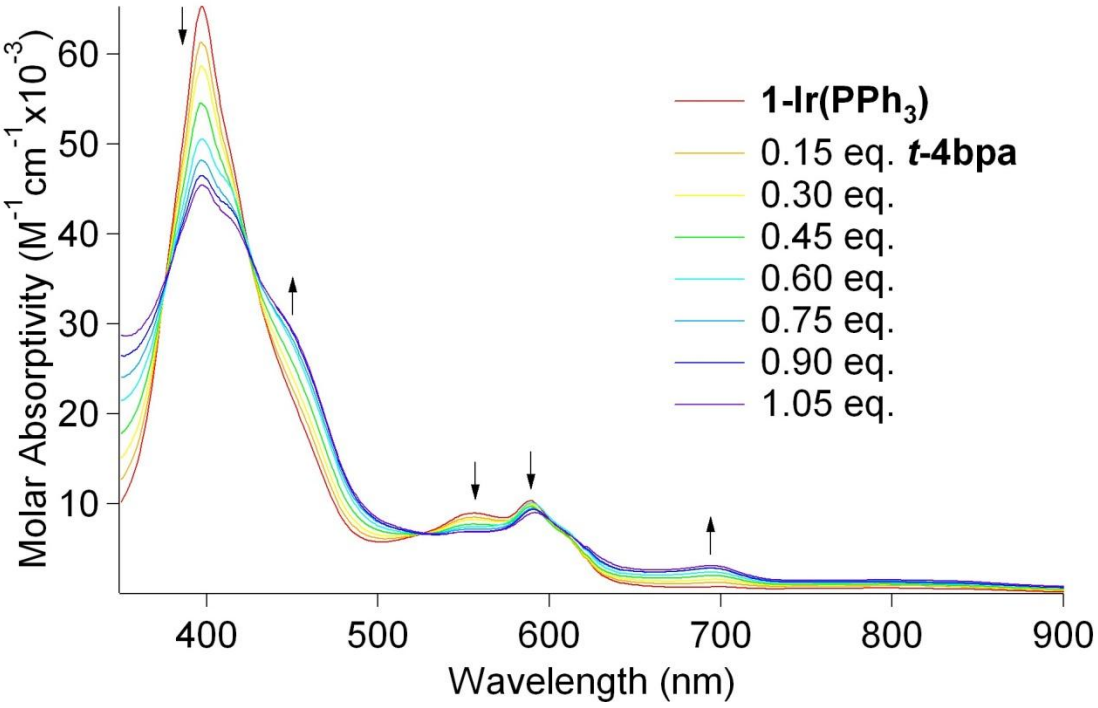
Molar Absorptivity (M-1cm-1x10-3)
Wavelength (nm)
1-Ir(PPh3)
0.15 eq. t-4bpa
0.30 eq.
0.45 eq.
0.60 eq.
0.75 eq.
0.90 eq.
1.05 eq.

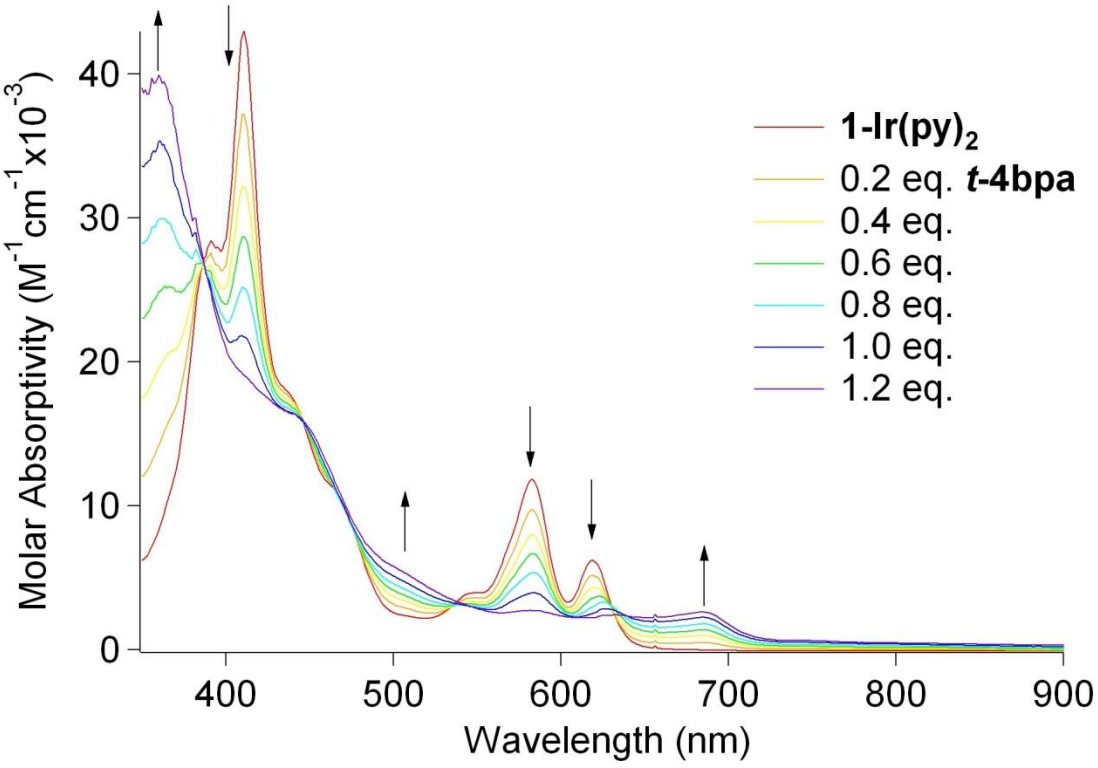
Molar Absorptivity (M-1cm-1x10-3)
Wavelength (nm)
1-Ir(py)2
0.2 eq. t-4bpa
0.4 eq.
0.6 eq.
0.8 eq.
1.0 eq.
1.2 eq.

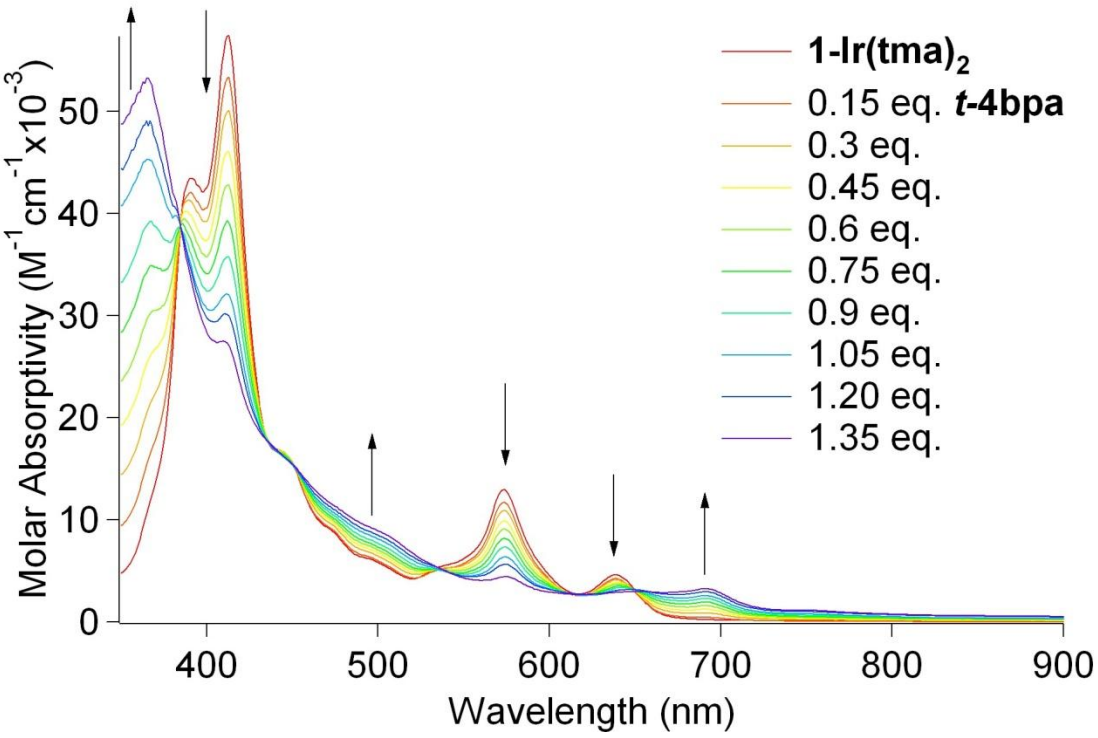

Figure 2-10: Absorption spectral changes accompanying oxidation of **1-Ir(PPh$_3$)** (top), **1-Ir(py)$_2$** (middle), and **1-Ir(tma)$_2$** by ***t*-4bpa**

EPR spectra. Carbon-based organic radicals, such as those obtained from oxidation of corrole complexes with non-redox-active metals like gallium(III), exhibit EPR spectra with isotropic *g* values near 2.0023.[30] In stark contrast, low-spin d^5 metal complexes with organic ligands display highly anisotropic EPR signals, often with hyperfine splittings attributable to electron-nucleus interactions.[36]

Complexes **1-Co(py)$_2$**, **1-Rh(py)$_2$**, **1-Ir(py)$_2$**, and **1-Ir(tma)$_2$** were oxidized chemically with 5 equivalents of elemental iodine in CH_2Cl_2, and EPR spectra of the resultant solutions were recorded at 20 K. Each of the spectra of the oxidized cobalt and rhodium complexes displays a single, narrow band [centered at g = 2.008 (Co, Figure 2-11a) or g = 2.003 (Rh, Figure 2-11b), respectively] clearly attributable to a corrole-based radical.

Such a radical signature is not found in the EPR spectrum of either of the oxidized **1-Ir(py)$_2$** and **1-Ir(tma)$_2$** complexes. The oxidation product of **1-Ir(tma)$_2$** (Figure 2-11c) exhibits a highly rhombic spectrum, with g tensor components (g_{zz} = 2.489, g_{yy} = 2.010 g_{xx} = 1.884) that are very similar to those of low-spin d^5 metalloporphyrinoids such as bis-amine-iron(III) porphyrins[37] and **1-Fe(py)$_2$**,[38] thereby demonstrating the presence of a *bona fide* iridium(IV) corrole. The spectrum of the product of oxidation of 1-Ir(py)$_2$ under the same conditions also is highly anisotropic, albeit with less rhombicity, with g_{zz} = 2.401, g_{yy} = 2.000, g_{xx} = 1.937 (Figure 2-11d).

Interpretation of the EPR spectra of oxidized five-coordinate complexes 1-Co(PPh$_3$), 1-Rh(PPh$_3$), and 1-Ir(PPh$_3$) is problematic. Oxidized 1-Co(PPh$_3$) and 1-Rh(PPh$_3$) appear to be corrole radicals (with isotropic g tensors centered near the free-electron value), but the electronic structure of oxidized 1-Ir(PPh$_3$) cannot be assigned, as its EPR spectrum is obscured by signals likely generated from side reactions with iodine.

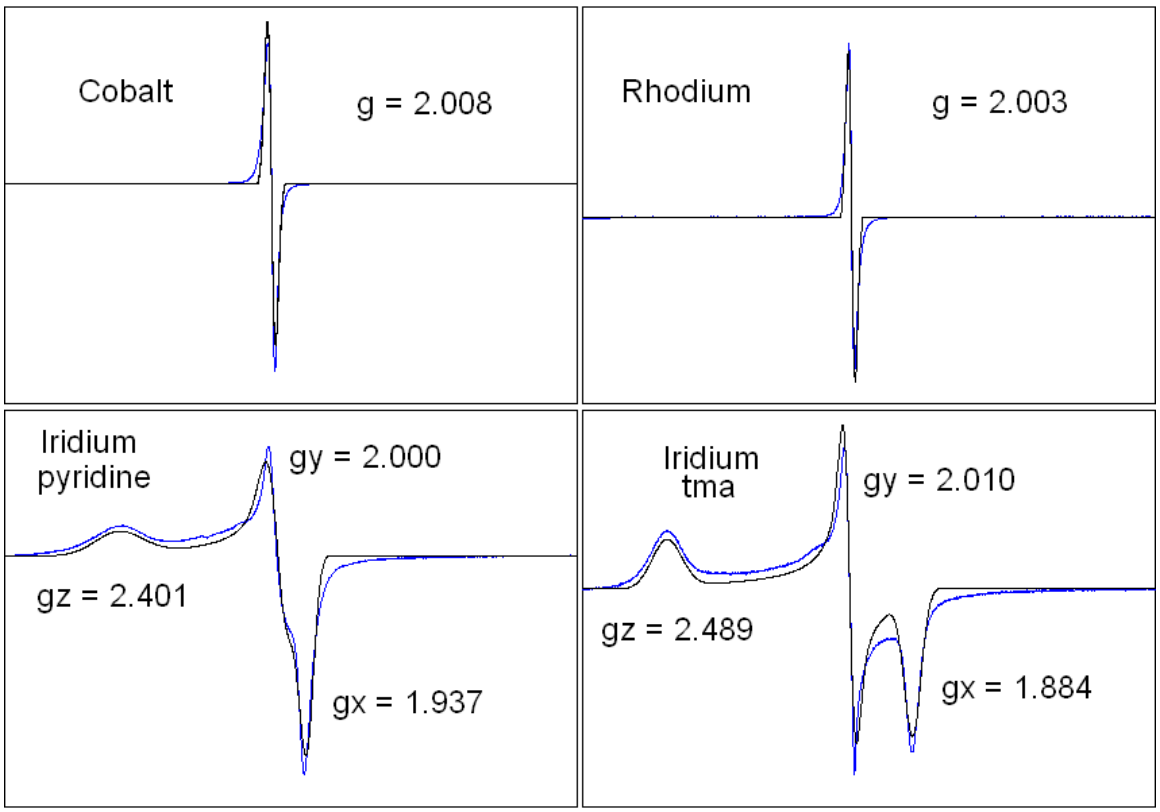

Figure 2-11: EPR spectra taken at 20 K in frozen toluene solutions (CH_2Cl_2 was added to Co and Rh toluene solutions with ***t*-4bpa**) of the chemically oxidized forms of (clockwise from top left): (a) **1-Co(py)$_2$**; (b) **1-Rh(py)$_2$**; (c) **1-Ir(tma)$_2$**; (d) **1-Ir(py)$_2$**. The blue traces are experimental spectra; the black traces are simulations performed using the SPINCOUNT package.

Concluding Remarks

Our investigation is the first to focus on the reactivity patterns of an isostructural series of corrole-chelated transition metals. The results shed new light on the chemical reactivity and stability of high oxidation states of metallocorroles. There is a clear trend within each series in terms of ligand substitution (only cobalt(III) corroles appear labile at room temperature) and ligand addition to the five-coordinate **1-M(PPh$_3$)** (Co < Rh < Ir), whereas all complexes display similar reduction potentials. The unexpected insensitivity of reduction potentials to metal identity has been interpreted in terms of different centers of oxidation for each complex. Absorption and EPR spectral data demonstrate that the

first oxidation is corrole-centered for cobalt and rhodium, but metal-centered for iridium. Our demonstration that the reactivity patterns of Ir(III) corroles are so different from those of 3d and 4d analogues suggests that increased efforts should be made to obtain complexes of other 5d metals, as it is likely that such materials will exhibit rich and in some cases unexpected physical and chemical properties that will further expand the range of useful applications for these electronically unique macrocycles.

Acknowledgment

This work was supported by the Center for Chemical Innovation Grant NSF CHE-0802907, US-Israel BSF (ZG and HBG), BP, CCSER (Gordon and Betty Moore Foundation), and the Arnold and Mabel Beckman Foundation. We thank Dr. Angelo Di Bilio for help with measurements of low-temperature EPR spectra; and Drs. Lawrence M. Henling and Michael W. Day for assistance with the acquisition and analysis of crystallographic data.

References

(1) a) Gross, Z.; Galili, N.; Saltsman, I. *Angew. Chem. Int. Ed.* **1999**, *38*, 1427–1429. b) Paolesse, R.; Jaquinod. L.; Nurco, D. J.; Mini, S.; Sagone, F.; Boschi, T.; Smith, K. M. *Chem. Commun.* **1999**,1307–1308. c) Gross, Z.; Galili, N.; Simkhovich, L.; Saltsman, I.; Botoshansky, M.; Blaser, D.; Boese, R.; Goldberg, I. *Org. Lett.* **1999**, *1*, 599–602. d) Koszarna, B.; Gryko, D.T. *J. Org. Chem.* **2006**, *71*, 3707–3717.

(2) a) Gryko, D. T. *J. Porphyrins Phthalocyanines*, **2008**, 12, 906. b) Nardis, S.; Monti, D.; Paolesse, R. *Mini–Rev. Org. Chem.* **2005**, *2*, 355–372.

(3) a) Aviv, I.; Gross, Z. *Chem. Commun.* **2007**, 1987–1999. b) Goldberg, D. P. *Acc. Chem. Res.* **2007**, *40*, 626–634. c) Gryko, D. T.; Fox, J. P.; Goldberg, D. P. *J. Porphyrins and Phthalocyanines* **2004**, *8*, 1091–1105.

(4) Simkhovich, L.; Gross, Z. *Tet. Lett.* **2001**, *42*, 8089–8092.

(5) a) Gross, Z.; Golubkov, G.; Simkhovich, L. *Angew. Chem. Int. Ed. Eng.* **2000**, *39*, 4045–4047. b) Golubkov, G.; Bendix, J.; Gray, H. B.; Mahammed, A.; Goldberg, I.; DiBilio, A. J.; Gross, Z. *Angew. Chem. Int. Ed. Eng.* **2001**, *40*, 2132–2134. c) Mandimutsira, B. S.; Ramdhanie, B.; Todd, R. C.; Wang, H. L.; Zareba, A. A.; Czemuszewicz, R. S.; Goldberg, D. P. *J. Am. Chem. Soc.* **2002**, *124*, 15170–15171.

(6) Mahammed, A.; Gray, H. B.; Meier–Callahan, A. E.; Gross, Z. *J. Am. Chem. Soc.* **2003**, *125*, 1162–1163.

(7) Grodkowski, J.; Neta, P.; Fujita, E.; Mahammed, A.; Simkhovich, L.; Gross, Z. *J. Phys. Chem. A*. **2002**, *106*, 4772–4778.
(8) a) Gross, Z.; Gray, H. B. *Comm. Inorg. Chem.* **2006**, *27*, 61. b) Hocking, R. K.; DeBeer George, S.; Gross, Z.; Walker, F. A.; Hodgson, K. O.; Hedman, B.; Solomon, E. I. *Inorg. Chem.* **2009**, *48*, 1678–1688.
(9) a) Golubkov, G.; Gross, Z. *Angew. Chem. Int. Ed.* **2003**, *42*, 4507–4510. b) Golubkov, G.; Gross, Z. *J. Am. Chem. Soc.* **2005**, *127*, 3258–3259.
(10) a) Gross, Z.; Gray, H.B. *Adv. Synth. Catal.* **2004**, *346*, 165–170. b) Mahammed, A.; Gross, Z. *Angew. Chem. Int. Ed.* **2006**, *45*, 6544–6547. c) Agadjanian, H.; Weaver, J. J.; Mahammed, A.; Rentsendorj, A.; Bass, S. ;Kim, J.; Dmochowski, I. J.; Margalit, R.; Gray, H. B.; Gross, Z.; Medina–Kauwe, L. K. *Pharm. Res.* **2006**, *23*, 367–377. d) Haber, A.; Mahammed,. A.; Fuhrman, B.; Volkova, N.; Coleman, R.; Hayek, T.; Aviram, M.; Gross, Z. *Angew. Chem. Int. Ed.* **2008**, *47*, 7896–7900.
(11) Flamigni, L.; Gryko, D. T. *Chem. Soc. Rev.* **2009**, *in press*.
(12) Agadjanian, H.; Ma, J.; Rensendorj, A.; Valluripalli, V.; Hwang, J. Y.; Mahammed, A.; Farkas, D. L.; Gray, H. B. *Proc. Natl. Acad. Sci. USA* **2009**, *106*, 6105–6110.
(13) Bruckner, C.; Barta, C. A.; Brinas, R. P.; Krause Bauer, J. A. *Inorg. Chem.* **2003**, *42*, 1673–1680.
(14) Simkhovich, L.; Luobeznova, I.; Goldberg, I.; Gross, Z. *Chem. Eur. J.* **2003**, *9*, 201–208.
(15) Saltsman, I.; Simkhovich, L.; Balazs, Y.; Goldberg, I.; Gross, Z. *Inorg. Chim. Acta* **2004**, *357*, 3038–3046.
(16) Luobeznova, I.; Raizman, M.; Goldberg, I.; Gross, Z. *Inorg. Chem.* **2006**, *45*, 386–394.
(17) Tse, M. K.; Zhang, Z.; Mak, T. C. W.; Chan, K. S. *Chem. Commun.* 1998, 1199–1200.
(18) Palmer, J. H.; Day, M. W.; Wilson, A. D.; Henling, L. M.; Gross, Z.; Gray, H. B. *J. Am. Chem. Soc.* **2008**, *130*, 7786–7787.
(19) a) Gryko, D. T.; Fox, J. P.; Goldberg, D. P. *Journal of Porphyrins and Phthalocyanines* **2004**, *8*, 1091–1105. b) Goldberg, D. P. *Acc. Chem. Res.* **2007**, *40*, 626–634. c) Kerber, W. D.; Goldberg, D. P. *J. Inorg. Biochem.* **2006**, *100*, 838–857. d) Aviv, I.; Gross, Z. *Chem. Commun.* **2007**, 1987–**1999**. e) Ghosh, A.; Steene, E. *J. Inorg. Biochem.* **2002**, *91*, 423–436. f) Kadish, K. M.; Shen, J.; Fremond, L.; Chen, P.; El Ojaimi, M.; Chkounda, M.; Gros, C. P.; Barbe, J. M.; Ohkubo, K.; Fukuzumi, S.; Guilard, R. *Inorg. Chem.* **2008**, *47*, 6726–6737.
(20) a) Cheung, C. W.; Chan, K. S. *Organometallics* **2008**, *27*, 3043–3055. b) Li, B.; Chan, K. S. *Organometallics* **2008**, *27*, 4034–4042. c) Cui, W.; Li, S.; Wayland, B. B. *J. Organomet. Chem.* **2007**, *692*, 3198–3206. d) Yanagisawa, M.; Tashiro, K.; Yamasaki, M.; Aida, T. *J. Am. Chem. Soc.* **2007**, *129*, 11912–11913. e) Song, X.; Chan, K. S. *Organometallics* **2007**, *26*, 965–970. f) Deng, Y.; Huang, M.–J. *Chem. Phys.* **2006**, *321*, 133–139. g) Toganoh, M.; Konagawa, J.; Furuta, H. *Inorg. Chem.* **2006**, *45*, 3852–3854. h) Flamigni, L.; Marconi, G.; Dixon, I. M.; Collin, J.–P.; Sauvage, J.–P. *J. Phys. Chem. B* **2002**, *106*, 6663–6671. i) Zhai, H.; Bunn, A.; Wayland B. *Chem. Commun*. **2001**, 1294–1295. j) Shi, C.; Mak, K. W.; Chan, K. S.; Anson, F. C. *J. Electroanal. Chem.*1995, *397*, 321–324. k) Collman, J. P.; Chng, L. L.; Tyvoll, D. A. *Inorg. Chem.* **1995**, *34*, 1311 – 1324. l) Kadish, K. M.; Deng, Y. J.; Yao, C.–L.; Anderson, J. E. *Organometallics* **1988**, 7, 1979–1983.
(21) Abbreviations: $[Ir(cod)Cl]_2$, H_3(tpfc), tpfc, Br_8–tpfc, ***t–4bpa***, tma–N–oxide, tma, and py stand for iridium(I) cyclooctadiene chloride dimer, 5,10,15–*tris*–pentafluorophenylcorrole, 5,10,15–*tris*–pentafluorophenylcorrolato trianion, 2,3,7,8,12,13,17,18–octabromo–5,10,15–*tris*–pentafluorophenylcorrolato trianion, *tris*(4–bromophenyl)aminium hexachloroantimonate, trimethylamine N–oxide, trimethylamine, and pyridine, respectively.
(22) Ou, Z.; Shao, J.; D'Souza, F.; Tagliatesta, P.; Kadish, K.M. *J. Porphyrins Pthalocyanines* **2004**, *8*, 201–214, and references therein.
(23) Kadish, K. M.; Shen, J.; Fremond, L.; Chen, P.; El Ojaimi, M.; Chkounda, M.; Gros, C. P.; Barbe, J. M.; Ohkubo, K.; Fukuzumi, S.; Guilard, R. *Inorg. Chem.* **2008**, *47*, 6726–6737.
(24) Brown, G. M.; Hopf, F. R.; Meyer, T. J.; Whitten, D. G.; *J. Am. Chem. Soc.* **1975**, *97*, 5385–5390.
(25) 140 μL of a solution of 0.5 mL of trifluoroacetic acid in 5 mL of CH_2Cl_2 was added to 1.73 mL of warm (liquid) pentafluorobenzaldehyde, with rapid stirring. Addition of 1.46 mL of freshly distilled pyrrole resulted in the rapid formation of a viscous red solution. After 10 minutes, 20 mL of CH_2Cl_2 was added and the mixture was allowed to stir briefly, followed by slow addition of 3.84 g of DDQ to oxidize the newly formed macrocycle. Purification was accomplished by successive chromatographic treatments

with 6.5:3.5 CH_2Cl_2:hexanes and 8.5:1.5 CH_2Cl_2:hexanes on silica, followed by recrystallization from hot pentane.
(26) a) Simkhovich, L.; Galili, N.; Saltsman, I.; Goldberg, I.; Gross, Z. *Inorg. Chem.* **2000**, *39*, 2704–2705. b) Mahammed, A.; Giladi, I.; Goldberg, I.; Gross, Z. *Chem. Eur. J.* **2001**, *7*, 4259–4265.
(27) Analogous procedures were employed for the synthesis of iridium(III) corroles with substituted pyridines; characterization data are reported in Supporting Information.
(28) Balazs, Y. S.; Saltsman, I.; Mahammed, A.; Tkachenko, E.; Golubkov, G.; Levine, J.; Gross, Z. *Magn. Reson. Chem.* **2004**, *42*, 624–635
(29) Simkhovich, L.; Goldberg, I.; Gross, Z. *J. Porphyrins Phthalocyanines.* **2002**, *6*, 439–444
(30) Bendix, J.; Dmochowski, I. J.; Gray, H. B.; Mahammed, A.; Simkhovich, L.; Gross, Z. *Angew. Chem. Int. Ed.* **2000**, *39*, 4048–4051.
(31) Kowalska, D.; Liu, X.; Tripathy, U.; Mahammed, A.; Gross, Z.; Hirayama, S.; Steer, R. P. *Inorg. Chem.* **2009**, *48*, 2670–2676.
(32) Calogero, G.; Giufridda, G.; Serroni, S.; Ricevuto, V.; Campagna, S. *Inorg. Chem.* **1995**, *34(3)*, 541–545.
(33) Gross, Z. *J. Biol. Inorg. Chem.* **2001**, *6*, 733–738.
(34) Fuhrhop, J. H.; Kadish, K. M.; Davis, D. G. *J. Am. Chem. Soc.* **1973**, *95*, 5140–5147.
(35) Meier–Callahan, A. E.; di Bilio, A. J.; Simkhovich, L.; Mahammed, A.; Goldberg, I.; Gray, H. B.; Gross, Z. *Inorg. Chem.* **2001**, *40*, 6788–6793.
(36) a) Diversi, P.; Iacoponi, S.; Ingrosso, G.; Laschi, F.; Lucherini, A.; Pinzino, C.; Ucello–Barretta, G.; Zanello, P. *Organometallics* **1995**, *14*, 3275–3287. b) Diversi, P.; de Biani, F. F.; Ingrosso, G.; Laschi, F.; Lucherini, A.; Pinzino, C.; Ucello–Barretta, G.; Zanello, P. *J. Organomet. Chem.* **1999**, *584*, 73–86.
(37) Walker, F. A. *Coord. Chem. Rev.* **1999**, *185–186*, 471–534.
(38) Simkhovich, L.; Goldberg, I.; Gross, Z. *Inorg. Chem.* **2002**, *41*, 5433–5439.